ELSEVIER

Cardiovascular Research 65 (2005) 104–116

Cardiovascular Research

www.elsevier.com/locate/cardiores

Comparison of ion channel distribution and expression in cardiomyocytes of canine pulmonary veins versus left atrium

Peter Melnyk, Joachim R. Ehrlich, Marc Pourrier, Louis Villeneuve, Tae-Joon Cha, Stanley Nattel*

Research Center, Montreal Heart Institute, 5000 Belanger Street East, Montreal, Quebec, Canada H1T 1C8
Departments of Pathology and Pharmacology and Therapeutics, McGill University and Department of Medicine, University of Montreal, Canada

Received 10 March 2004; received in revised form 30 July 2004; accepted 16 August 2004
Available online 19 September 2004
Time for primary review 20 days

Abstract

Background: Cardiomyocytes in pulmonary vein (PV) sleeves are important in atrial fibrillation (AF), but underlying mechanisms are poorly understood. Pulmonary veins have different ionic current properties compared to left atrium, with pulmonary vein inward-rectifier currents being smaller and delayed-rectifier currents larger than in left atrium.
Methods: Expression and distribution of the inward-rectifier subunits Kir2.1 and Kir2.3, the rapid delayed-rectifier α-subunit ERG, the slow delayed-rectifier α-subunit KvLQT1, the β-subunit minK, the L-type Ca^{2+}-subunit $Ca_v1.2$, and the Na^+,Ca^{2+}-exchanger were quantified by Western blot on isolated cardiomyocytes and localized by immunohistochemistry in tissue sections obtained from canine hearts.
Results: Western blotting indicated significantly greater expression of ERG (by 28%, $P<0.05$) and KvLQT1 (by 34%, $P<0.05$) in pulmonary vein versus left atrial (LA) cardiomyocytes, but smaller Kir2.3 and similar Kir2.1, $Ca_v1.2$ and Na^+,Ca^{2+}-exchanger expression in PV. Kir2.1 exhibited weak transverse tubular distribution in both regions. Kir2.3 localized to intercalated disks in both regions, and to transverse tubules in left atrium but not pulmonary vein. ERG staining was more intense in pulmonary vein than left atrium, localizing to transverse tubules in both regions and intercalated disks in pulmonary veins. KvLQT1 was more intensely expressed in pulmonary veins, with a transverse tubular and intercalated disk localization, versus a more diffuse signal in left atrium. The Na^+,Ca^{2+}-exchanger localized to transverse tubules, plasma membranes and intercalated disks with similar intensity in each region.
Conclusions: Greater ERG and KvLQT1 abundance in pulmonary vein cardiomyocytes, lower abundance of Kir2.3 in pulmonary veins and differential pulmonary vein subcellular distribution of Kir2.3, ERG and KvLQT1 subunits may contribute to ionic current differences between pulmonary vein and left atrial cardiomyocytes.

Keywords: Arrhythmia (mechanisms); ECG; Ion channels; Repolarization

1. Introduction

The triggering of atrial fibrillation (AF) paroxysms by cardiac tissue around the pulmonary veins (PVs) [1,2], in conjunction with the success of PV catheter-ablation treatment for AF [3–5], has underlined the importance of understanding the mechanisms by which PV cardiomyocyte sleeves are implicated in atrial arrhythmogenesis. The extensive clinical literature regarding the role of PVs in AF contrasts with much more limited knowledge of the basic electrophysiological properties of PV cardiomyocytes and how these promote arrhythmia generation [6]. Compared to left atrial (LA) myocytes, PV sleeve cardiomyocytes have distinct electrophysiological proper-

* Corresponding author. Research Center, Montreal Heart Institute, 5000 Belanger Street East, Montreal, Quebec, Canada H1T 1C8. Tel.: +1 514 376 3330; fax: +1 514 376 1355.
E-mail address: nattel@icm.umontreal.ca (S. Nattel).

0008-6363/$ - see front matter © 2004 European Society of Cardiology. Published by Elsevier B.V. All rights reserved.
doi:10.1016/j.cardiores.2004.08.014

ties related to different densities of several ionic currents [7]. The mechanisms for these ionic current differences are unknown. One possible mechanism is a difference in ion channel subunit expression. This study tested the hypothesis that protein subunits composing I_{K1}, I_{Kr} and I_{Ks} channels are differentially distributed in the PV cardiomyocyte sleeve compared to LA free wall. Because PVs are composed of a variety of tissues, including cardiomyocyte sleeves along with venous adventitia, media and intima, we performed Western blot analysis on isolated PV cardiomyocytes to minimize contamination from other cell types, and used immunohistochemistry to study the intracellular distribution of cardiomyocyte proteins in situ.

2. Methods

2.1. Animal and tissue handling

Adult mongrel dogs of either sex were anesthetized with pentobarbital (30 mg/kg^{-1} iv) and artificially ventilated. Animal handling procedures followed Canadian Council on Animal Care guidelines, were consistent with National Institutes of Health guidelines and were approved by the institutional Animal Research Ethics Committee.

Atrial cell isolation was performed as previously described [8]. Hearts and adjacent lung tissue were excised via left thoracotomy, and were then immersed in oxygenated Tyrode solution. For PV cardiomyocyte isolation, the proximal circumflex coronary artery was cannulated and the distal ends of PV myocardial sleeves were marked with silk thread to aid in their identification after collagenase (100 U ml^{-1}, Worthington, type II) digestion. Following digestion (~ 45 min), the epicardial tissues were removed. PV cardiomyocytes were well digested, whereas the smooth muscle layer was not. Rod-shaped PV cardiomyocytes with cross striations were isolated from all PVs. PV cells were typically isolated 4–10 mm from the ostium. Cells for Western blot study were stored at 4 °C for no more than 2 h.

2.2. Immunohistochemistry and confocal imaging

PV and LA tissues were dissected, immersed in isobutanol cooled to −80 °C and stored for later use. Serial 14-μm sections were cut perpendicular to the long axis of the veins at −20 °C with a Leica CM19000 cryostat and dried before storage (−80 °C). Tissue sections were fixed for 20 min with 3% paraformaldehyde. Tissues were permeabilized with 0.5% Triton X-100 and blocked with 10% normal goat serum (NGS, Jackson Immuno-Research Laboratories) or, for KvLQT1, 10% normal donkey serum (NDS, Jackson Immuno-Research Laboratories) and incubated overnight at 4 °C with primary antibodies: anti-Kir2.1 1:500, anti-Kir2.3 1:500, anti-ERG 1:450, anti-minK 1:250 (all polyclonal, raised in rabbit; all purchased from Alomone Labs), anti-KvLQT1 1:500 (polyclonal, raised in goat; purchased from Santa Cruz) or anti-NCX 1:500 (polyclonal, raised in rabbit; purchased from RDI). Primary antibodies were diluted in phosphate-buffered saline (PBS) with 0.1% Triton X-100 and 2% normal goat serum (or normal donkey serum for KvLQT1). For double-labeling experiments, tissues were incubated with wheat germ agglutinin (WGA) conjugated with Oregon green 488 (Molecular Probes) after primary antibody removal. After three washes with PBS, secondary antibodies (goat anti-rabbit IgG-Cy3 or donkey anti-goat IgG-Cy5 (for KvLQT1 labeling, Jackson Immuno-Research Laboratories)) were applied (45 min, room temperature). Following three additional washes, the sections were mounted using immunofluore (ICN Biomedicals).

Sections were imaged with a Zeiss LSM-510 inverted confocal microscope. To observe Cy3-labeling (excitation: 553 nm, emission: 575 nm), a 543-nM HeNe laser was used; to record Cy5 labeling (excitation: 651 nm, emission: 674 nm), a 633-nM HeNe laser was applied.

2.3. Protein extraction

Membrane proteins were extracted from isolated PV and LA cardiomyocytes. After isolation, cells were centrifuged at 1000×g for 5 min. The supernatant was discarded and the cells were resuspended in lysis buffer. The suspension was homogenized and centrifuged at 1000×g to pellet cellular debris, and then the remaining supernatant was centrifuged at 45,000×g at 4 °C for 20 min. The pellet was resuspended in resuspension buffer. Total protein concentration was determined by Bradford assay and samples were stored in resuspension buffer at −80 °C.

2.4. Protein electrophoresis and Western blotting

Samples were loaded on 8% polyacrylamide gels in an alternating PV-LA pattern. Following electrophoretic separation, proteins were transferred to polyvinilidine-difluoride membranes (Millipore). After transfer, membranes were blocked with 5% nonfat dry milk (NFDM) in tris-buffered saline (TBS) with 0.1% Tween 20 (TTBS). Primary antibodies (anti-Kir2.1, anti-Kir2.3, anti-KvLQT1 (1:1000), anti-ERG (1:750), anti-NCX (1:1000), anti-Ca_v1.2 (1:500) and anti-minK (1:750)) were diluted with 1% NFDM in TTBS and incubated with membranes overnight at 4 °C. This was followed by three washes in TTBS and re-blocking of membranes with 1% NFDM in TTBS. Secondary antibodies were diluted in 5% NFDM and applied to membranes for 45 min at room temperature. The membranes were washed in TTBS prior to incubation with Western Lightning Chemiluminescence Reagent-Plus (Perkin-Elmer Life Sciences) and film exposure. Band density was measured with Quantity One software (PDI) and background subtraction algorithms. Protein loading was

controlled by probing Western blots with anti-GAPDH (RDI) and normalizing ion channel protein band intensities to GAPDH values.

Lysis buffer consisted of (mM) Tris–HCl (5) pH 7.4, EDTA (2) and included 10 μg/ml benzamidine, 5 μg/ml leupeptin and 5 μg/ml soybean trypsin inhibitor. Resuspension buffer contained (mM) Tris–HCl (75) pH 7.4, EDTA (2) and $MgCl_2$ (12.5) in addition to protease inhibitors.

2.5. Cell transfection

Chinese hamster ovary (CHO) cells were cultured at 37 °C with 5% CO_2 in supplemented F12 medium (GIBCO). Cells were transfected with 1 μg cDNA (KvLQT1, ERG, minK, Kir2.1 or Kir2.3) subcloned into pcDNA3, along with 0.1 μg GFP cDNA, which served as an indicator of successful transfection, 5.5 μl of Lipofectamine (GIBCO) and 6 μl of Plus reagent, added to DMEM to a final volume of 200 μl, then added to 800-μl cell suspension. After 6-h incubation at 37 °C and 5% CO_2, 1 ml of 20% FBS was added to provide a final FBS concentration of 10%. Following overnight incubation, the cells were re-plated for 2 additional days in culture. After transfection, CHO cells were incubated at 37 °C for 1 h on laminin-coated (15 μg/ml) glass coverslips, then fixed with 2% paraformaldehyde, blocked with 5% normal goat serum (Jackson ImmunoResearch) or 5% normal donkey serum (Jackson ImmunoResearch) and permeabilized with 0.2% Triton X-100. The primary antibodies were applied for overnight incubation at 4 °C. After washing with PBS, the cells were incubated with the secondary antibody for 45 min at room temperature.

2.6. Electrophysiological recordings

After enzymatic isolation, single PV and LA cardiomyocytes were stored in a high K^+ solution as previously described. (8) Ionic currents were recorded with whole-cell patch-clamp at 36±0.5 °C using an Axopatch 200 B amplifier and pClamp software (V6.0, Axon). Borosilicate glass electrodes had 1.5–3 MΩ tip resistances when filled with internal solution containing (mM): K-aspartate 110, KCl 20, $MgCl_2$ 1, MgATP 5, GTP (lithium salt) 0.1, HEPES 10, Na-phosphocreatine 5 and EGTA 5.0 (pH 7.3 with KOH) and immersed in external solution (Tyrode) containing (mM): NaCl 136, KCl 5.4, $MgCl_2$ 1, $CaCl_2$ 1, NaH_2PO_4 0.33, HEPES 5 and dextrose 10 (pH 7.35 with NaOH). For K^+ current (I_{Ks}, I_{Kr}, I_{K1}) recordings, nifedipine (5 μM), 4-aminopyridine (2 mM) and atropine (200 nM) were added to suppress I_{Ca}, transient-outward current (I_{to}) and 4-aminopyridine-dependent muscarinic K^+ currents. I_{Ks} was recorded as dofetilide (1 μM)-resistant current and I_{Kr} tail currents were recorded as chromanol 293 B (50 μM)-resistant current. The external and internal solutions for I_{NCX} recordings were as previously published [7]. For I_{NCX} recording, niflumic acid 0.1 mM and nifedipine 5 μM were added [7]. Mean compensated cell capacitances were 86±6 and 87±6 pF for PV and LA cardiomyocytes, respectively (n=26, 37, P=ns). Mean compensated series resistances were 3.6±0.1 (PV) vs. 3.7±0.2 (LA) MΩ (P=ns).

2.7. Data analysis

Comparisons between group means were by Student's t-test. The results are given as mean±S.E.M. and two-tailed $P<0.05$ was considered statistically significant. Clampfit (Axon Instruments) and GraphPad Prism V3.0 were used for analysis of electrophysiological data.

3. Results

3.1. Electrophysiological recordings

Representative electrophysiological recordings are shown, along with voltage protocols and mean±S.E.M. densities, in Fig. 1. I_{Ks} tail-current density was significantly greater in PV cardiomyocytes (panel A). I_{Kr} was also significantly larger in PV (panel B). In contrast, I_{K1} density was significantly smaller in PV (panel C), whereas I_{NCX} was comparable in PV and LA (panel D).

3.2. Antibody specificity against subunits expressed in transfected cells

Since our primary tools were antibodies directed against ion channel subunits, we began by expressing the subunits in CHO cells and probing each subunit with a panel of antibodies to ensure specificity. Fig. 2 shows cells transfected with one delayed-rectifier subunit and probed with antibodies directed against each of the delayed-rectifier subunits. Each transfected cell is shown as a pair of images: a GFP-stained (green) immunofluorescent image to the left and antibody-directed immunofluorescence (red positive staining) to the right. Cells transfected with each subunit stained positively only with antibodies directed towards that subunit, with no cross-reactivity from other antibodies. Fig. 3A and B shows corresponding data for inward-rectifier subunits, along with data from cells transfected with minK and KvLQT1, which did not react with anti-Kir2.1 or 2.3. Fig. 3C shows that the anti-NCX antibody did not react with ion channel subunits.

3.3. Quantification of ion channel subunit protein by Western blot

Representative Western blots of the inward rectifier subunits, Kir2.1 and Kir2.3, are shown in Fig. 4. The Kir2.1 antibody detected a single clear band of molecular weight ~59 kDa (lanes 1 and 2, Fig. 4A). Similarly, the

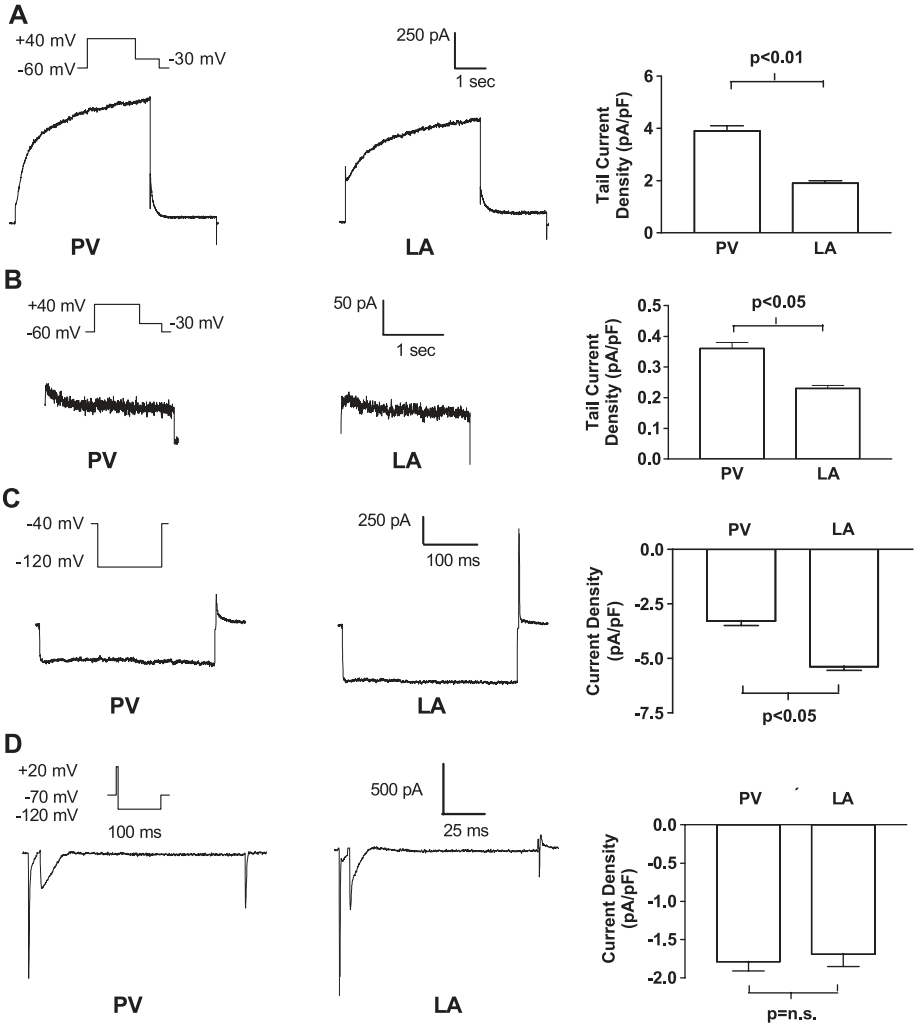

Fig. 1. Examples of currents recorded from isolated LA and PV cardiomyocytes. Representative PV recordings are presented at the left of each panel, LA recordings in the middle, mean±S.E.M. current densities (n=10 cells/observation), at the test potential indicated in each panel, to the right. Voltage protocols are shown in insets. (A) Recordings of I_{Ks} during 2-s depolarization to +40 mV followed by repolarization to −30 mV. (B) Chromanol 293B-resistant tail currents recorded with the same protocol as in A. (C) Representative barium-sensitive inward-rectifier currents. (D) I_{NCX} obtained by subtracting recordings from a cell before and after removal of external Na^+ by equimolar Li^+ substitution.

Kir2.3 antibody detected a single ~62-kDa band (lanes 1 and 2, Fig. 4B). Anti-GAPDH detected a single band of molecular weight ~34 kDa for each sample as shown. Channel subunit band intensities for each sample were normalized to corresponding GAPDH band intensity on the same gel, then normalized to corresponding LA samples and expressed as a percentage of the LA signal. Mean values for subunit expression in both regions are shown in panel C. PV Kir2.1 expression was 95% of LA values (P=ns). Kir2.3 abundance was significantly lower in PVs than LA (PV Kir2.3=81% LA Kir2.3, P<0.05).

Western blot results for the delayed-rectifier subunits KvLQT1, ERG and minK in LA and PV cardiomyocytes are illustrated in Fig. 5. The KvLQT1 antibody detected a prominent band of molecular weight ~55 kDa (arrow, panel A). Signal intensity was greater in PV than LA samples. The ERG antibody detected a prominent band at ~165 kDa (arrow), which was stronger in PV cardiomyocytes (panel B). The minK antibody revealed a prominent band at ~30 kDa (panel C). Mean±S.E.M. data for all experiments are shown in panel D. Overall, PV KvLQT1 band intensity was ~34% greater than LA (P<0.05) and ERG intensity was also greater in PV, by ~28% (P<0.05). MinK expression was comparable in both regions (PV minK averaged 111% of LA minK, P=ns).

Typical Western blot results for the Na^+,Ca^{2+}-exchanger are shown in Fig. 6. The bands of interest (arrows) are seen at 160, 120 and 70 kDa. Similar NCX bands in cardiac tissue have been described in several previous studies [9,10]. McDonald et al. [10] identified these three bands as containing amino acid residues 371–525 of NCX and quantified regional NCX expression by summing immunosignals from each band for a given region. We proceeded similarly. NCX subunit expression was comparable in the two cell types (PV NCX=106% LA NCX, P=ns). $Ca_v1.2$, the α1-c subunit of the L-type calcium channel, was

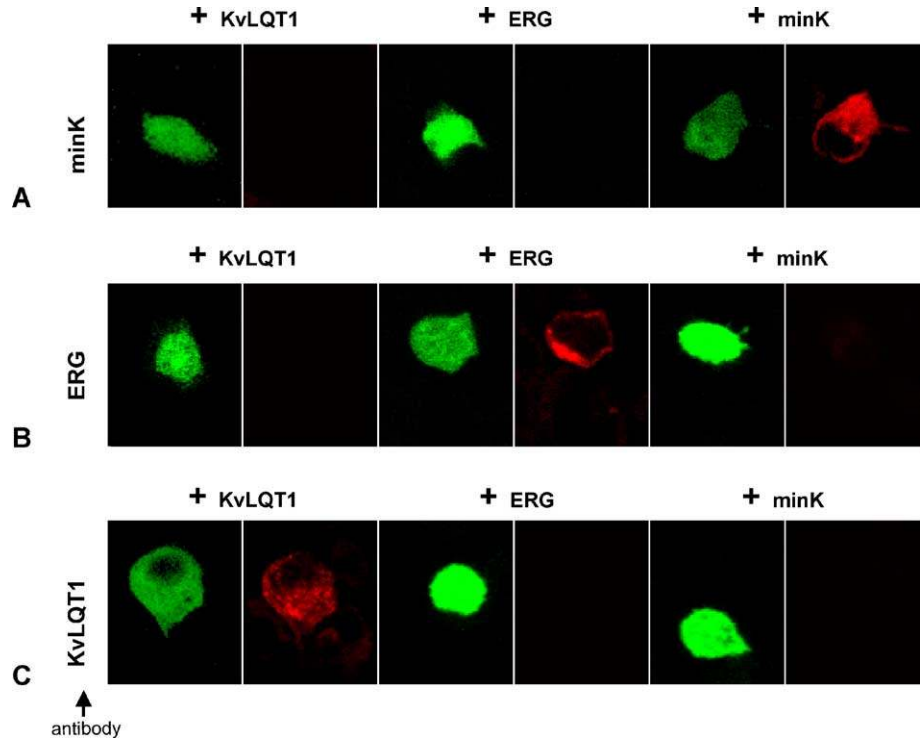

Fig. 2. Studies of reactivity of antibodies with CHO cells expressing delayed-rectifier K^+ channel subunits. The transfected constructs are listed above each panel. Antibody probes are indicated at the left. (A) CHO cells transiently transfected with KvLQT1, ERG or minK probed with anti-minK. (B, C) KvLQT1, ERG or minK transfected cells incubated with anti-ERG (B) or anti-KvLQT1 (C). Similar results were obtained in four experiments each with KvLQT1, ERG and minK expressing cells.

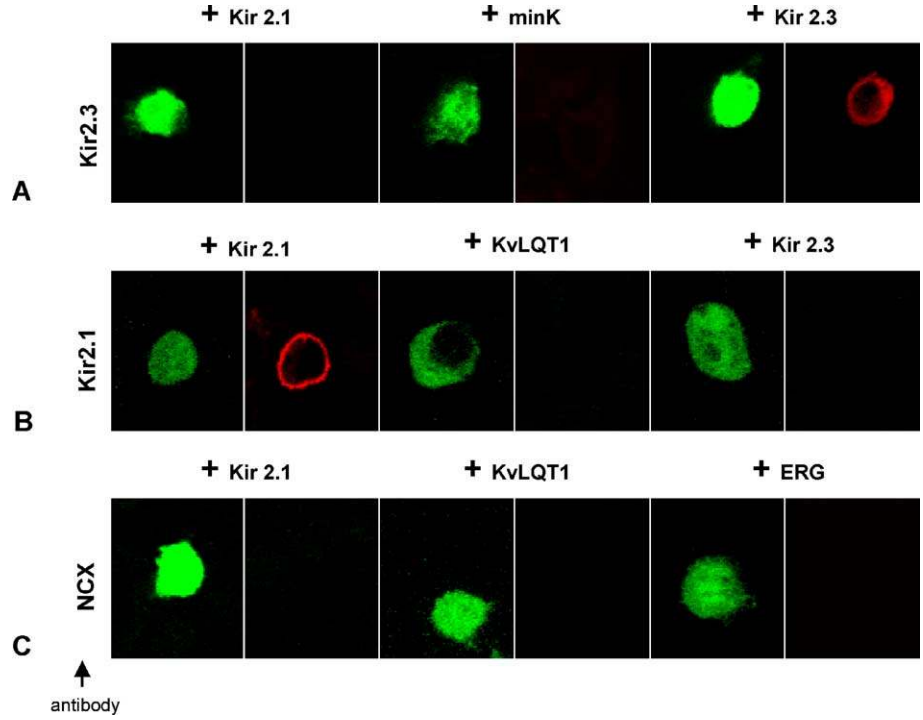

Fig. 3. Studies of reactivity of antibodies with CHO cells expressing inward-rectifier K^+ channel subunits. (A) CHO cells transiently transfected with Kir2.1, minK and Kir2.3 incubated with anti-Kir2.3. (B) CHO cells transfected with Kir2.1, KvLQT1 and Kir2.3 and incubated with anti-Kir2.1. (C) CHO cells transfected with Kir2.1, KvLQT1 and ERG and incubated with anti-NCX. Similar results were obtained in four experiments each of the type shown in panels A, B and C.

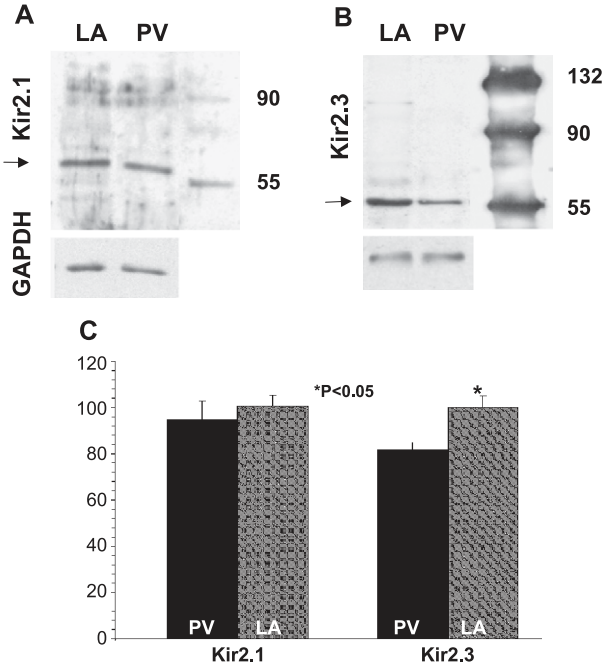

Fig. 4. Kir2.1 (A) and Kir2.3 (B) expression levels as determined by Western blotting. GAPDH expression is shown below each respective immunoblot. Lanes 1 and 2, LA and PV samples; lane 3, molecular weight marker. (C) mean±S.E.M. expression levels of Kir2.1 and Kir2.3 in PV and LA myocytes (n=5 blots in LA and 5 blots in PV for Kir2.1 and Kir2.3).

detected as a strong signal at ~205 kDa (Fig. 7). The expression of $Ca_v1.2$ was found to be similar in PV and LA cardiomyocytes (PV $Ca_v1.2$=94% LA $Ca_v1.2$, P=ns).

3.4. Immunohistochemistry

The Western blot results provide a potential explanation for observed differences in delayed-rectifier current density between PV and LA, since ERG and KvLQT1 band intensity were both stronger in PV than LA, implying stronger membrane expression of these proteins. Consistent with the smaller I_{K1} density in PV compared to LA cardiomyocytes, one of the inwardly rectifying subunits (Kir2.3) was less strongly expressed by Western blot, although the principal I_{K1} subunit, Kir2.1, was similar between regions. We used immunohistochemistry to examine further the subcellular distribution of inward-rectifier, delayed-rectifier and Na^+,Ca^{2+}-exchanger subunits in PV and LA tissues in situ. Fig. 8 illustrates the subcellular distribution of the inward-rectifier subunits Kir2.1 and Kir2.3 in LA and PV tissue sections. Kir2.1 exhibited a similar weak cross-striated localization in both PV (panel A) and LA (panel B) cardiomyocytes. We have previously shown that this localization in canine cardiac tissue corresponds to transverse tubules [12] and is relatively weak in atrial tissues. Kir2.3 was only observed at the intercalated disks of PV myocytes (panel C), but showed a strong signal at intercalated disks and transverse tubules of LA (panel D).

The subcellular distributions of the delayed-rectifier subunits minK, KvLQT1 and ERG are shown in Fig. 9. MinK was primarily localized at intercalated disks in both PV (panel A) and LA (panel B) tissue. In PV, strong ERG signals were seen in a cross-striated distribution, as well as at cell

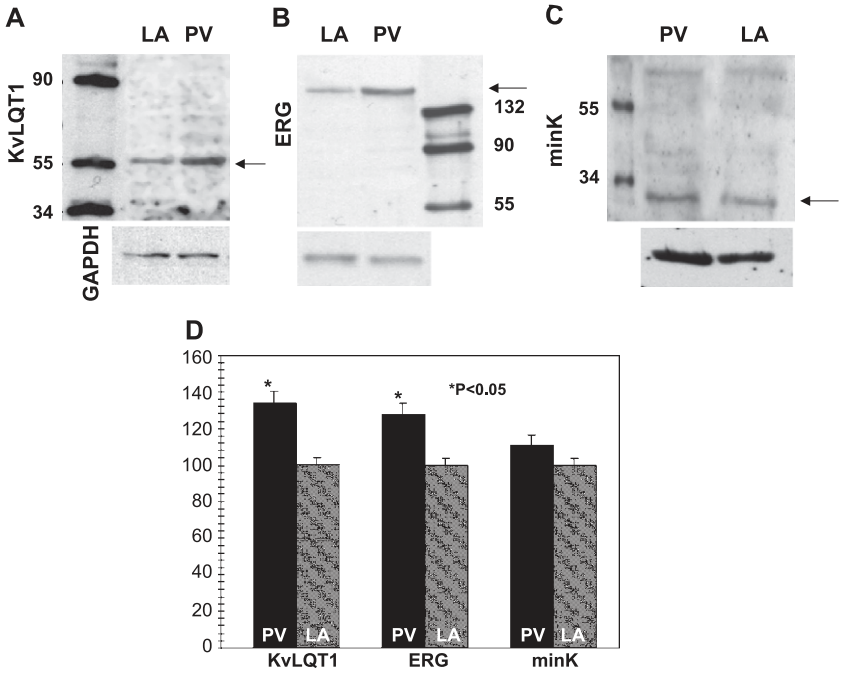

Fig. 5. Representative Western blot results for KvLQT1 (A), ERG (B) and minK (C) expression in PV and LA myocytes. Left lanes show molecular weight markers, middle and right lanes are LA and PV samples, respectively. GAPDH signals are shown below each respective immunoblot. (D) Mean±S.E.M. expression levels of KvLQT1, ERG and minK in PV and LA myocytes (n=5 blots in LA and 5 blots in PV for each subunit). *P<0.05 between PV and LA band densities.

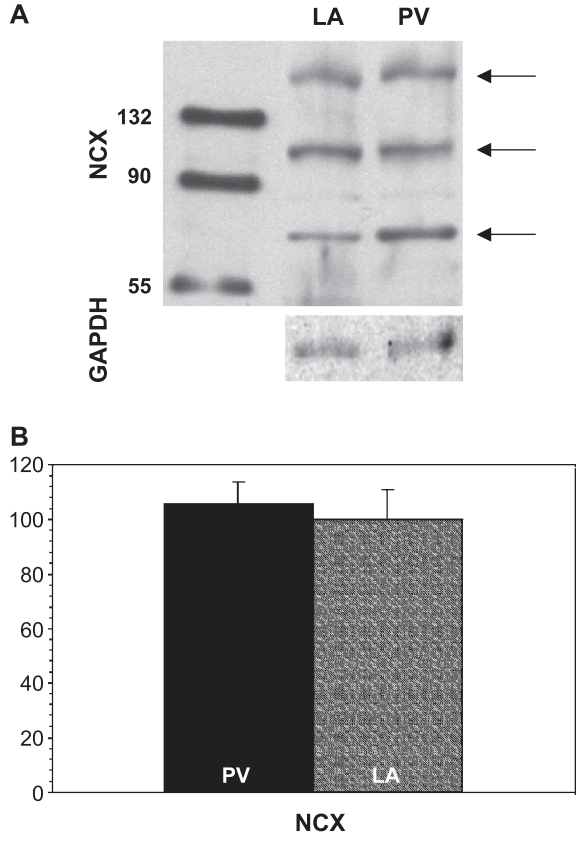

Fig. 6. (A) NCX Western blots in PV and LA myocytes. Molecular weight markers are shown at the left. Bands of expected molecular weight for NCX (160, 120 and 70 kDa) are indicated by arrows. GAPDH bands are shown below each corresponding NCX blot. (B) Bar graph comparing PV and LA NCX expression levels (n=5 blots each for LA and PV).

ends at a location compatible with intercalated disks (panel C). The ERG signal was much weaker in LA (panel D), and the power of the HeNe laser had to be increased to identify clearly the cross-striated, but not cell-end, ERG distribution. In PV cardiomyocytes, the KvLQT1 signal was strong and located in both cross-striated and cell-end patterns (panel E). The KvLQT1 signal in LA was weak and diffuse with fewer striations (panel F). NCX subunit protein was detected in cross-striations, at cell ends and in lateral membranes in both PV and LA cardiomyocytes (Fig. 10A and B). Negative controls (consisting of pre-incubating the antigenic peptide with the antibody for anti-Kir2.1, Kir2.3, ERG, KvLQT1 and minK, and omitting the primary antibody for NCX) all resulted in loss of signals (data not shown).

To determine the relationship between cross-striated patterns and transverse tubules, double labeling experiments were performed with WGA, a transverse tubule marker [11] and NCX, KvLQT1 and ERG. Fig. 11 shows representative images of a PV cardiomyocyte labeled with anti-NCX (panel A) and WGA (panel B). The composite image is shown in panel C. The yellow color indicates co-localization. KvLQT1 (red, panel D) and wheat germ agglutinin (blue, panel E) also co-localized (purple, panel F). The striated ERG distribution (panel G) also paralleled WGA labeling (panel H), with the corresponding composite image shown in panel I. Thus, the cross-striated pattern seen for these antibodies corresponds to transverse tubules, as previously shown for Kir2.1 and 2.3 [12]. Fig. 12 shows co-localization of N-cadherin (an intercalated disk marker) with ERG (top), NCX (middle) and Kir2.3 (bottom) staining in PV tissue. The results indicate that cell-end staining corresponds to an intercalated disk distribution.

4. Discussion

We have found differential expression and subcellular distribution of ion channel subunits involved in the formation of inward and delayed-rectifier K^+ channels between LA and PV cardiomyocytes. These differences correspond qualitatively to differences in ion current densities.

4.1. Cellular electrophysiological properties of PVs in relation to present findings

Ehrlich et al. [7] demonstrated that PV cardiomyocytes have distinct electrophysiological properties compared to

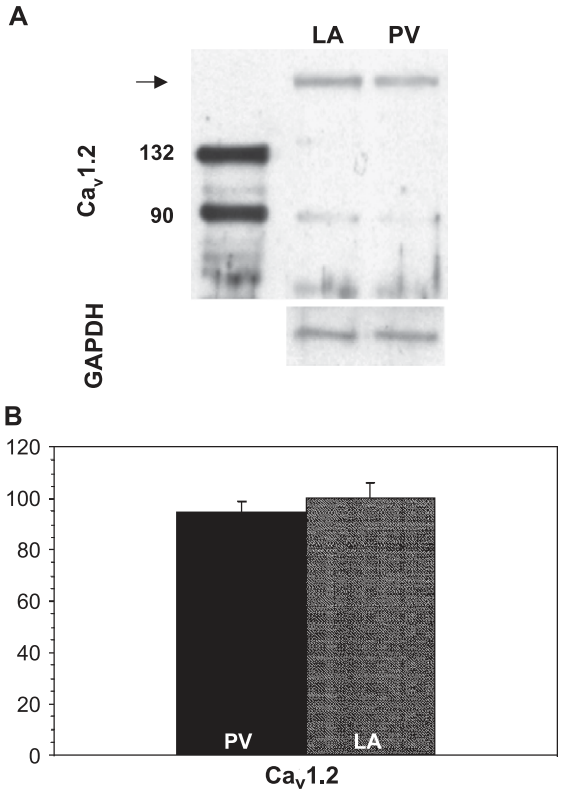

Fig. 7. Representative Western blot results for $Ca_v1.2$ expression in PV and LA myocytes. (A) The left lane shows molecular weight markers and the middle and right lanes are LA and PV samples respectively. GAPDH bands are shown below each respective immunoblot. (B) Mean±S.E.M. expression levels of $Ca_v1.2$ in PV and LA myocytes (n=5 blots in LA and 5 blots in PV for each subunit).

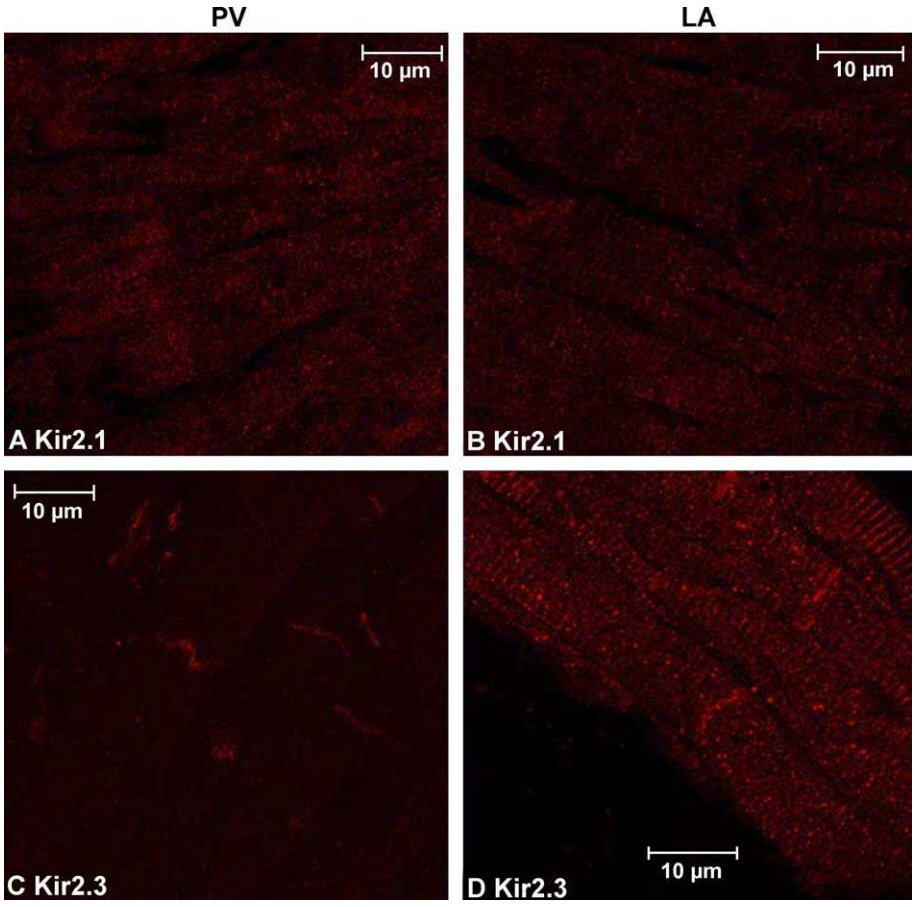

Fig. 8. Immunohistochemical determination of the distribution of inwardly rectifying subunits. (A, B) Immunolocalization of Kir2.1 in canine PV (A) and LA (B) myocytes. (C, D) Kir2.3 localization in PV (C) and LA (D) myocytes. Similar results were obtained in five hearts for LA and five hearts for PV probed with Kir2.1 and Kir2.3 antibodies.

LA cells. Differences included smaller phase-0 upstroke velocity (V_{max}), less negative resting potential and shorter action potential duration (APD) in PVs. Ionic current differences were noted between PV and LA cardiomyocytes, with smaller PV I_{K1} believed to contribute to the decreased PV resting potential and larger I_{Kr} and I_{Ks} contributing to shorter APD. Although the molecular basis of I_{K1} is not completely understood, Kir2 subunits, including Kir2.1 and Kir2.3, are believed to play an important role [12]. We found Kir2.1 and Kir2.3 to be expressed in both LA and PV cardiomyocytes. The protein expression and subcellular distribution of Kir2.1 was similar in both regions. However, Kir2.3 was expressed at a lower overall level in PV and the subcellular distribution of Kir2.3 was quite different in PV cardiomyocyte sleeves versus LA free wall, with cell-end staining corresponding to intercalated disks seen in both but striated staining corresponding to transverse tubules observed only in LA. The lack of transverse tubular Kir2.3 localization in PV cardiomyocytes may potentially contribute to their smaller I_{K1} density. The transverse tubular system has been implicated in depolarization spread through the cell [13] and several ion channels have been localized to the transverse tubular system [11,14]. We previously noted differences in subcellular distribution of Kir2.1 and 2.3 between LA and left ventricular myocardial tissue, with ventricle showing much stronger Kir2.1 transverse tubular staining and LA showing stronger Kir2.3 transverse tubular staining [12]. Since atrial-ventricular differences in overall Kir2-subunit expression by Western blot were insufficient to account for ion current density differences, it was suggested that subcellular distribution differences might be an important contributor [12]. Similarly, the lesser transverse tubular distribution of Kir2.3 subunits in PV cardiomyocytes compared to LA may contribute to their smaller I_{K1}. This contrasts with the apparent role of Kir2.1 in LA-left ventricular I_{K1} differences.

The ether-a-go-go related gene *ERG* has been identified as the molecular basis of I_{Kr} [15,16]. Canine ERG shows 97% amino acid homology to the human counterpart [17]. The presence of intercalated disk and more intense transverse tubular ERG distribution in PV cardiomyocytes compared with LA is consistent with their larger I_{Kr}. These findings are further supported by the Western blot data indicating significantly stronger expression of this subunit in PV. I_{Kr} is an important determinant of APD [15,18,19]. The differential distribution of ERG in PV

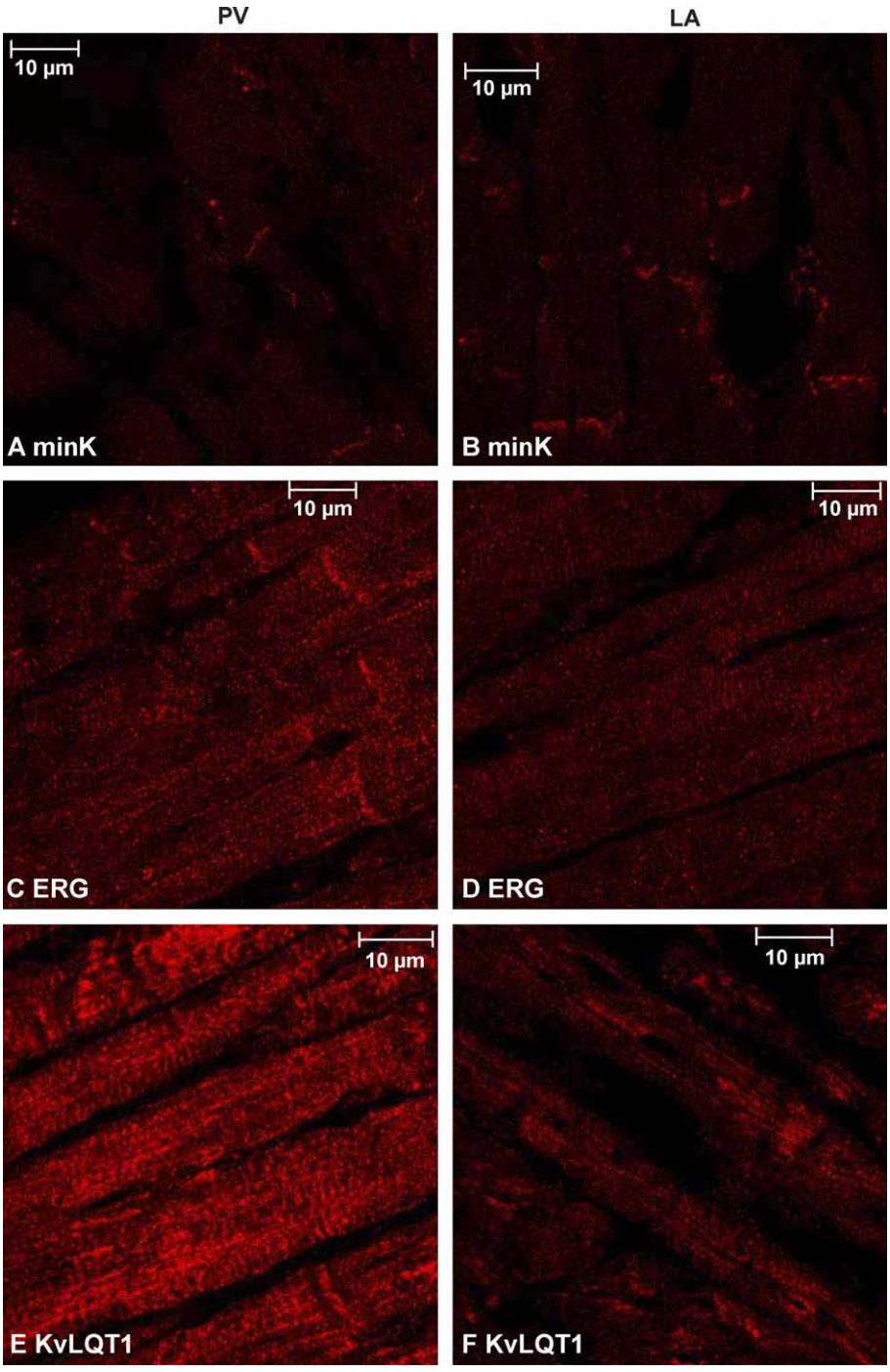

Fig. 9. The subcellular distribution of delayed-rectifier subunits. (A, B) MinK distribution in PV (A) and LA (B) myocytes. (C, D) ERG localization in PV (C) and LA (D) myocytes. PV (E) and LA (F) KvLQT1 localization is shown in panels E and F. Similar results were obtained in five hearts for LA and five hearts for PV with Kir2.1 minK, ERG and KvLQT1 antibodies.

cardiomyocytes may therefore contribute to the shorter APD in PVs [7].

The pore of I_{Ks} channels is formed by KvLQT1 subunits, which interact with minK to form functional I_{Ks} [20]. In addition to the more defined, transverse tubular and intercalated disk distribution of KvLQT1 in PVs, Western blot results indicated a stronger overall expression in PVs compared to LA. These differences likely contribute to the greater PV I_{Ks} density. Like I_{Kr}, I_{Ks} has also been shown to influence repolarization [21,22], particularly in the presence of prominent β-adrenergic stimulation [22], and variations in I_{Ks} can contribute significantly to ventricular action potential heterogeneity [23]. Thus, PV-LA differences in I_{Ks} density and subcellular distribution may contribute to their distinct repolarization properties.

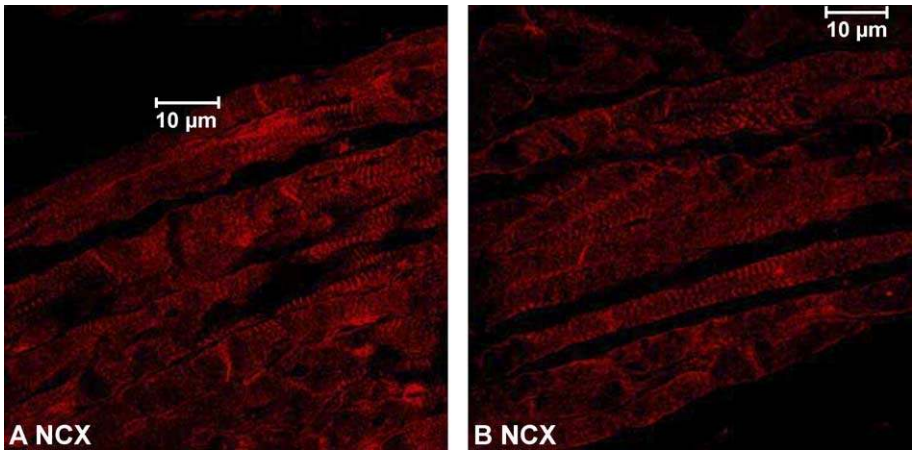

Fig. 10. NCX distribution in PV (A) and LA (B). Similar results were obtained in five hearts for LA and five hearts for PV, respectively.

I_{Ca} is smaller in PVs than LA [7]. Based on our Western blot studies, this difference is not due to differences in protein expression and may be due to differential regulation, e.g. by the autonomic nervous system and related signal transduction. Further work in this area would be of interest but is beyond the scope of the present study.

4.2. Electrophysiology of PVs and their role in AF

Electrical excitation spreads between the atrium and PVs [24–26]. The PVs are a critical source of ectopic foci triggering clinical AF [1,2,4] and may also be important in maintaining the arrhythmia [27]. Spontaneous transition from atrial flutter to AF may be initiated by PV ectopic foci [28]. Both focal [4] and circumferential [29] PV ablation are valuable in the treatment of AF. The precise mechanisms by which PVs contribute to the initiation and maintenance of AF are unclear and remain a subject of intense investigation [6].

Several distinct cellular electrophysiological properties of PV cardiomyocytes have been noted and suggested to contribute to their arrhythmogenic properties. Chen et al. [30] showed spontaneous pacemaker activity, as well as various forms of triggered activity, in canine PV cardiomyocytes, with activity enhanced by atrial remodeling [31]. Honjo et al. [32] described susceptibility of PV cardiomyocytes to triggered activity on exposure to the sarcoplasmic reticulum Ca^{2+} release channel blocker ryanodine. One possible basis for triggered activity, enhanced NCX activity, is made less likely by the observation that I_{NCX} is similar in PV and LA and that PV and LA NCX protein expression are similar.

In addition to sources of focal discharge, PVs may also be privileged sites for atrial reentry [33]. The anatomical structure of PVs involves discontinuities in fibre orientation that can produce important local conduction slowing [34,35]. In addition to their specific fibre orientation properties, PVs have a distinct distribution of connexins, with lower connexin-40 expression compared to LA, that may contribute to their particular conduction properties [36]. The cellular electrophysiological properties of PVs may also contribute to a role in reentry [7]. The less negative PV resting potential, apparently due to decreased I_{K1} [7], results in Na^+ channel inactivation and reduced V_{max} [7,33], potentially decreasing source current and causing conduction slowing. The shorter PV APD, due in part to larger delayed-rectifier currents [7], may limit refractoriness and favour initiation and maintenance of reentry.

In the present study, we assessed the potential molecular basis for differential I_{K1}, I_{Kr} and I_{Ks} properties of PV versus LA cardiomyocytes by studying the distribution of underlying ion channel subunits. Our observation of greater ERG and KvLQT1 expression in PV cells provides a potential explanation for observed differences in I_{Kr} and I_{Ks}. The lower expression level and different subcellular distribution of Kir2.3 protein may contribute to differences in I_{K1}. To our knowledge, the present study is the first analysis in the literature of ion channel subunit expression in PV cardiomyocytes, and provides potential explanations for some of their distinct and potentially significant cellular electrophysiological properties.

4.3. Potential limitations

The analysis of PV cardiomyocyte protein expression is complicated by the fact that only a thin sleeve of myocardial tissue surrounds the proximal PVs. Thus, particular care is needed to ensure that any analysis is not contaminated by non-cardiac tissue from other components of the PVs. We dealt with this by using isolated cardiomyocytes for Western blot studies and by using immunohistochemistry of intact PV sections in which the underlying anatomy could be clearly defined. Ion current density can be influenced by cell isolation and it is conceivable that ion channel subunit protein expression might be affected by the isolation procedure. Since comparisons were made between isolated LA and PV

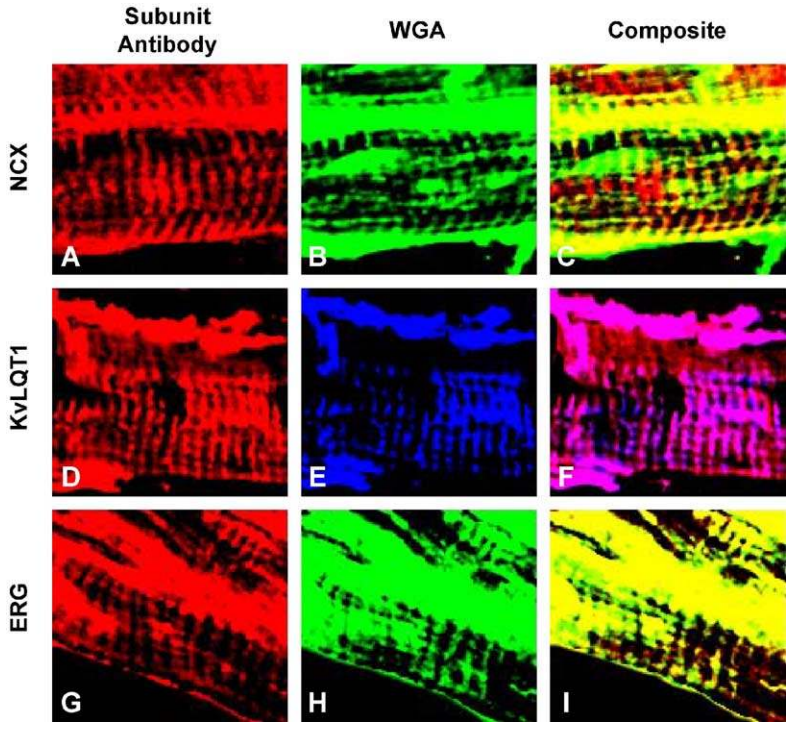

Fig. 11. WGA co-localization experiments. PV NCX expression (A) and WGA labeling (B). The compound image is in panel C. (D, E) KvLQT1 and WGA distributions, respectively. (F) Composite image. (G, H) ERG and WGA localization. The composite image is in panel I. Similar results for each subunit were obtained in tissue sections from three hearts.

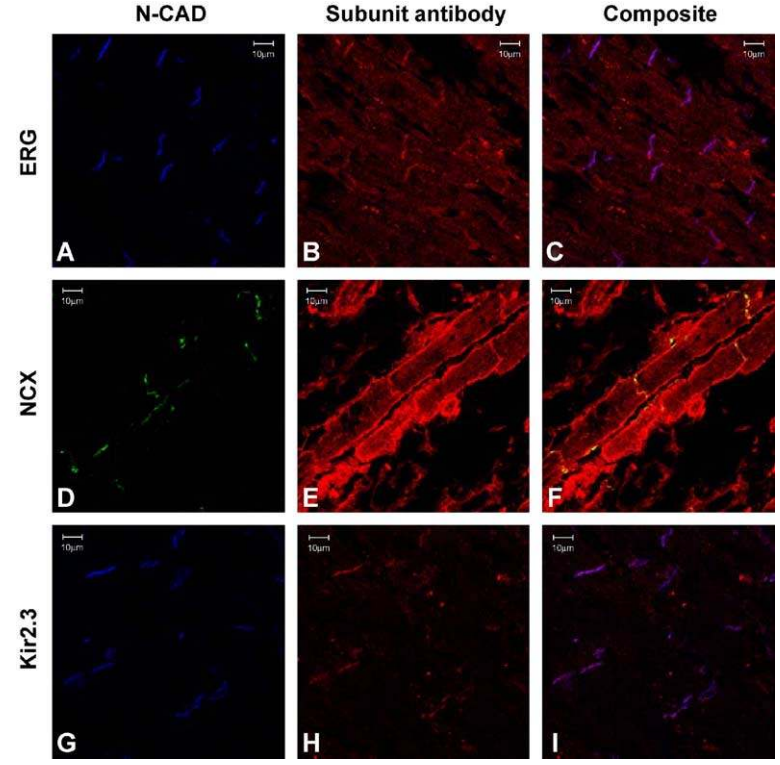

Fig. 12. Co-localization experiments with N-cadherin (N-CAD). PV N-cadherin expression (A) and ERG labeling (B). The composite image is in panel (C). (D, E) PV N-cadherin and NCX distributions, respectively. (F) Composite image. (G) PV N-cadherin and (H) Kir 2.3 localization. The composite image is in panel (I).

cardiomyocytes, the effects of isolation should affect both cell types similarly. Furthermore, tissues subjected to immunohistochemical analysis were not subjected to cell isolation and the differential distribution of Kir2.3, KvLQT1 and ERG in PV versus LA was consistent with Western blot results.

Acknowledgements

The authors thank Evelyn Landry and Nathalie L'Heureux for technical assistance and Monique Brouillard and France Thériault for secretarial help. Funding was provided by the Canadian Institutes of Health Research and the Quebec Heart and Stroke Foundation. Peter Melnyk was supported by a Heart and Stroke Foundation of Canada Studentship.

References

[1] Haissaguerre M, Jais P, Shah DC, Takahashi A, Hocini M, Quiniou G, et al. Spontaneous initiation of atrial fibrillation by ectopic beats originating in the pulmonary veins. N Engl J Med 1998;339:659–66.
[2] Chen SA, Hsieh MH, Tai CT, Tsai CF, Prakash VS, Yu WC, et al. Initiation of atrial fibrillation by ectopic beats originating from the pulmonary veins: electrophysiological characteristics, pharmacological responses, and effects of radiofrequency ablation. Circulation 1999;100:1879–86.
[3] Haissaguerre M, Jais P, Shah DC, Garrigue S, Takahashi A, Lavergne T, et al. Electrophysiological end point for catheter ablation of atrial fibrillation initiated from multiple pulmonary venous foci. Circulation 2000;101:1409–17.
[4] Jais P, Haissaguerre M, Shah DC, Chouairi S, Gencel L, Hocini M, et al. A focal source of atrial fibrillation treated by discrete radiofrequency ablation. Circulation 1997;95:572–6.
[5] Pappone C, Rosanio S, Augello G, Gallus G, Vicedomini G, Mazzone P, et al. Mortality, morbidity, and quality of life after circumferential pulmonary vein ablation for atrial fibrillation: outcomes from a controlled nonrandomized long-term study. J Am Coll Cardiol 2003 Jul 16;42(2):185–97.
[6] Nattel S. Basic electrophysiology of the pulmonary veins and their role in atrial fibrillation: precipitators, perpetuators, and perplexers. J Cardiovasc Electrophysiol 2003;14:1372–5.
[7] Ehrlich JR, Cha TJ, Zhang L, Chartier D, Melnyk P, Hohnloser SH, et al. Cellular electrophysiology of canine pulmonary vein cardiomyocytes: action potential and ionic current properties. J Physiol (Lond) 2003;551:801–13.
[8] Li D, Zhang L, Kneller J, Nattel S. Potential ionic mechanism for repolarization differences between canine right and left atrium. Circ Res 2001;88:1168–75.
[9] Iwata T, Galli C, Dainese P, Guerini D, Carafoli E. The 70 kD component of the heart sarcolemmal Na+/Ca(2+)-exchanger preparation is the C-terminal portion of the protein. Cell Calcium 1995; 17:263–9.
[10] McDonald RL, Colyer J, Harrison SM. Quantitative analysis of Na^+–Ca^{2+} exchanger expression in guinea-pig heart. Eur J Biochem 2000; 267:5142–8.
[11] Takeuchi S, Takagishi Y, Yasui K, Murata Y, Toyama J, Kodama I. Voltage-gated K(+)Channel, Kv4.2, localizes predominantly to the transverse-axial tubular system of the rat myocyte. J Mol Cell Cardiol 2000;32:1361–9.
[12] Melnyk P, Zhang L, Shrier A, Nattel S. Differential distribution of Kir2.1 and Kir2.3 subunits in canine atrium and ventricle. Am J Physiol Heart Circ Physiol 2002;83:H1123–33.
[13] Vaughan PC, Howell JN, Eisenberg RS. The capacitance of skeletal muscle fibers in solutions of low ionic strength. J Gen Physiol 1972;59:347–59.
[14] Scriven DR, Dan P, Moore ED. Distribution of proteins implicated in excitation–contraction coupling in rat ventricular myocytes. Biophys J 2000;79:2682–91.
[15] Sanguinetti MC, Jiang C, Curran ME, Keating MT. A mechanistic link between an inherited and an acquired cardiac arrhythmia: HERG encodes the IKr potassium channel. Cell 1995;81:299–307.
[16] Trudeau MC, Warmke JW, Ganetzky B, Robertson GA. HERG, a human inward rectifier in the voltage-gated potassium channel family. Science 1995;269:92–5.
[17] Zehelein J, Zhang W, Koenen M, Graf M, Heinemann SH, Katus HA. Molecular cloning and expression of cERG, the ether a go-go-related gene from canine myocardium. Pflugers Arch 2001;442: 188–91.
[18] Cheng J, Kamiya K, Liu W, Tsuji Y, Toyama J, Kodama I. Heterogeneous distribution of the two components of delayed rectifier K^+ current: a potential mechanism of the proarrhythmic effects of methanesulfonanilideclass III agents. Cardiovasc Res 1999;43:135–47.
[19] Courtemanche M, Ramirez RJ, Nattel S. Ionic targets for drug therapy and atrial fibrillation-induced electrical remodeling: insights from a mathematical model. Cardiovasc Res 1999;42: 477–89.
[20] Sanguinetti MC, Curran ME, Zou A, Shen J, Spector PS, Atkinson DL, et al. Coassembly of K(V)LQT1 and mink (IsK) proteins to form cardiac I(Ks) potassium channel. Nature 1996;384:80–3.
[21] Bosch RF, Gaspo R, Busch AE, Lang HJ, Li GR, Nattel S. Effects of the chromanol 293B, a selective blocker of the slow, component of the delayed rectifier K^+ current, on repolarization in human and guinea pig ventricular myocytes. Cardiovasc Res 1998;38:441–50.
[22] Volders PG, Stengl M, van Opstal JM, Gerlach U, Spatjens RL, Beekman JD, et al. Probing the contribution of I_{Ks} to canine ventricular repolarization: key role for beta-adrenergic receptor stimulation. Circulation 2003;107:2753–60.
[23] Viswanathan PC, Shaw RM, Rudy Y. Effects of I_{Kr} and I_{Ks} heterogeneity on action potential duration and its rate dependence: a simulation study. Circulation 1999;99:2466–74.
[24] Spach MS, Barr RC, Jewett PH. Spread of excitation from the atrium into thoracic veins in human beings and dogs. Am J Cardiol 1972;30:844–54.
[25] Cheung DW. Electrical activity of the pulmonary vein and its interaction with the right atrium in the guinea-pig. J Physiol (Lond) 1981;314:445–56.
[26] Haissaguerre M, Shah DC, Jais P, Hocini M, Yamane T, Deisenhofer I, et al. Electrophysiological breakthroughs from the left atrium to the pulmonary veins. Circulation 2000;102:2463–5.
[27] Oral H, Knight BP, Tada H, Ozaydin M, Chugh A, Hassan S, et al. Pulmonary vein isolation for paroxysmal and persistent atrial fibrillation. Circulation 2002;105:1077–81.
[28] Hsieh MH, Tai CT, Tsai CF, Yu WC, Lin WS, Huang JL, et al. Mechanism of spontaneous transition from typical atrial flutter to atrial fibrillation: role of ectopic atrial fibrillation foci. Pacing Clin Electrophysiol 2001;24:46–52.
[29] Pappone C, Rosanio S, Oreto G, Tocchi M, Gugliotta F, Vicedomini G, et al. Circumferential radiofrequency ablation of pulmonary vein ostia: a new anatomic approach for curing atrial fibrillation. Circulation 2000;102:2619–28.
[30] Chen YJ, Chen SA, Chang MS, Lin CI. Arrhythmogenic activity of cardiac muscle in pulmonary veins of the dog: implication for the genesis of atrial fibrillation. Cardiovasc Res 2000;48:265–73.
[31] Chen YJ, Chen SA, Chen YC, Yeh HI, Chan P, Chang MS, et al. Effects of rapid atrial pacing on the arrhythmogenic activity of single

cardiomyocytes from pulmonary veins: implication in initiation of atrial fibrillation. Circulation 2001;104:2849–54.
[32] Honjo H, Boyett MR, Niwa R, Inada S, Yamamoto M, Mitsui K, et al. Pacing-induced spontaneous activity in myocardial sleeves of pulmonary veins after treatment with ryanodine. Circulation 2003;107:1937–43.
[33] Arora R, Verheule S, Scott L, Navarrete A, Katari V, Wilson E, et al. Arrhythmogenic substrate of the pulmonary veins assessed by high-resolution optical mapping. Circulation 2003;107:1816–21.
[34] Hocini M, Ho SY, Kawara T, Linnenbank AC, Potse M, Shah D, et al. Electrical conduction in canine pulmonary veins: electrophysiological and anatomic correlation. Circulation 2002;105:2442–8.
[35] Hamabe A, Okuyama Y, Miyauchi Y, Zhou S, Pak HN, Karagueuzian HS, et al. Correlation between anatomy and electrical activation in canine pulmonary veins. Circulation 2003;107:1550–5.
[36] Verheule S, Wilson EE, Arora R, Engle SK, Scott LR, Olgin JE. Tissue structure and connexin expression of canine pulmonary veins. Cardiovasc Res 2002;55:727–38.